Carrier-mediated magnetoelectricity in complex oxide heterostructures

James M. Rondinelli, Massimiliano Stengel, and Nicola A. Spaldin*

Materials Department, University of California,

Santa Barbara, CA, 93106-5050, USA

(Dated: June 18, 2007)

Abstract

The search for a general means to control the coupling between electricity and magnetism has intrigued scientists since Ørsted's discovery of electromagnetism in the early 19th century. While tremendous success has been achieved to date in creating both single phase and composite magnetoelectric materials, the quintessential electric-field control of magnetism remains elusive. In this work, we demonstrate a linear magnetoelectric effect which arises from a novel carrier-mediated mechanism, and is a universal feature of the interface between a dielectric and a spin-polarized metal. Using first-principles density functional calculations, we illustrate this effect at the $SrRuO_3/SrTiO_3$ interface and describe its origin. To formally quantify the magnetic response of such an interface to an applied electric field, we introduce and define the concept of spin capacitance. In addition to its magnetoelectric and spin capacitive behavior, the interface displays a spatial coexistence of magnetism and dielectric polarization suggesting a route to a new type of interfacial multiferroic.

The linear magnetoelectric effect is the first-order magnetic response of a system to an applied electric field, or equivalently the electrical polarization induced by an applied magnetic field[1,2]:

$$P_i = \alpha_{ij} H_j \tag{1}$$

$$M_i = \alpha_{ji} E_j \quad , \tag{2}$$

where α is the magnetoelectric tensor, which is non-zero in the absence of time-reversal and space-inversion symmetries. Although the effect has long been recognized both theoretically[3] and experimentally[4] it has traditionally been of only academic interest because of its inherent weakness in intrinsic single phase materials. The last few years, however, have seen a tremendous revival of activity in magnetoelectrics[2], motivated in large part by the entirely new device paradigms that would be enabled by electric-field-control of magnetism[5,6]. Progress has been fueled by the growth of novel single-phase[7,8] and composite[9,10] multiferroic materials, which show simultaneous magnetic and ferroelectric ordering and have the potential for significantly enhanced magnetoelectric responses.

Currently two mechanisms for magnetoelectric coupling are well established. In traditional single-phase magnetoelectrics, of which Cr_2O_3 is the prototype, an *intrinsic* magnetoelectric coupling occurs[3]. An electric field both shifts the positions of the magnetic cations relative to the anions – changing both the dipolar and exchange contributions to the magnetic interactions – and modifies the electronic wavefunctions, which further changes the magnetic coupling. This behavior, and its inverse when a magnetic field is applied, are enhanced in materials with strong spin-orbit coupling (and hence strong coupling of the magnetic order to the lattice) and with large piezo- or electro-strictive response. In composites of magnetostrictive or piezomagnetic materials combined with electrostrictive or piezoelectrics, an *extrinsic* magnetoelectric coupling is mediated by strain at the interface[9,11]. Here an electric field causes strain in the electrical component which is mechanically transferred to the magnetic component where it changes the magnetization (and vice versa)[44]. This class of structures appears very promising for technological applicability, in part because the underlying working principles are essentially based on the bulk properties of the constituents. Very accurate modeling has thus been achieved at the level of semiclassical theories[9], which has allowed for efficient opti-

mization of geometry and material properties.

Recently, it has been pointed out that thin film growth of heterostructures can be exploited to create structures which break inversion symmetry, even when the parent bulk materials are centrosymmetric[12]. In fact at the interface between any two unlike materials the space inversion symmetry is intrinsically broken. Therefore, provided that one of the two components breaks time-reversal symmetry (which occurs in the case of a ferromagnet), we should expect a linear magnetoelectric coupling to occur, even in the absence of a piezo- or electro-strictive material (Table I). An intriguing recent observation of electric-field tunable magnetization at the surface of a ferromagnetic electrode in an electro-chemical cell[13] may indeed be a manifestation of such an interfacial effect. Ref. 13 suggested an important role played by accumulation/depletion of carriers at the ferromagnetic surface, but a detailed microscopic mechanism could not be determined. A simpler and more convenient architecture for developing a quantitative and general model is a capacitor geometry, in which one of the two components of the bilayer is a metal and the other is an insulating dielectric, and a second electrode is deposited on top of the insulating film to provide a source of external bias; we study this geometry here.

The magnetoelectric response of such an interface is intimately related to the local details of chemistry, bonding, structure and electronics, which often strongly depart from those of single-phase compounds; to account for the subtle balance of these often competing factors requires a fully quantum-mechanical treatment. Density functional theory has proven to be a very effective tool to deal with the challenging problem of complex oxide interfaces; however, the lack of a rigorous methodological framework to treat finite electric fields in metal-insulator heterostructures has until recently thwarted attempts to access dielectric and magnetoelectric responses of such systems. Recent advances in finite electric field methods[14,15], which we extended in this work to include the magnetic degree of freedom, enables such calculations for the first time.

Here we demonstrate computationally a novel linear magnetoelectric effect which is *carrier-mediated* in origin. The effect occurs at the interface between a non-magnetic, nonpolar dielectric and a metal with spin-polarized carriers at the Fermi level. Using first-principles density functional theory, we find that

(i) an electric field induces a linear change in magnetization in the metal at the interface, with the sign of the change determined by the orientation of the applied field,

(ii) the magnetic response is mediated by the accumulation of spin-polarized charge within the few atomic layers closest to the interface; this charge is stored capacitively leading to a spintronic analogue to a traditional charge capacitor, and

(iii) as a result of the magnetoelectric response, magnetism and dielectric polarization coexist in the interfacial region, suggesting a route to a new type of *interfacial multiferroic*.

We choose $SrRuO_3/SrTiO_3$ heterostructures as our representative system, motivated by the favorable dielectric properties of $SrTiO_3$ (STO)[16] and the widespread use of thin film ferromagnetic $SrRuO_3$ (SRO) as oxide electrodes[17]; furthermore, the effects of interfacial carrier modulation in thin films of both materials have been intensively investigated as a possible route to the realization of novel field-effect devices[18,19]. We note that our conclusions are not specific to this system but should apply to any dielectric/magnetic metal interface. Since such interfaces are similar to those already in place for magnetic tunnel junctions[20], rapid experimental verification of this effect should be well within reach.

Our calculations are performed within the local spin-density approximation (LSDA) of density functional theory and the projector-augmented wave[21] (PAW) method[45], with a planewave basis cutoff energy of 40 Ry. Our model heterostructure consists of seven unit cells of $SrRuO_3$ periodically alternating with seven unit cells of $SrTiO_3$ (Figure 1) along the (100) direction. The in-plane lattice parameter was set to the theoretical $SrTiO_3$ equilibrium lattice constant (3.85 Å) to simulate epitaxial growth on a $SrTiO_3$ substrate. The two-dimensional Brillouin zone of the resulting tetragonal cell was sampled with six special k-points, corresponding to a 6×6 Monkhorst-Pack mesh[22]. The ion positions and out-of-plane lattice constants were fully relaxed until the forces on the ions and the out-of-plane stress were less than 1 meV $Å^{-1}$ using an extension of the Car and Parrinello method for metallic systems[23,24,25]. To study dielectric and magnetoelectric responses we used a spin-polarized extension of our recently developed method for applying finite electric fields to metal-insulator heterostructures[14,15]. With these parameters we obtain structural, dielectric and electronic properties for bulk $SrTiO_3$ and $SrRuO_3$ that are consistent with earlier theoretical studies[26,27,28,29]. In particular, our calculated dielectric constant for cubic $SrTiO_3$ at this lattice constant is $\epsilon = 490$, in excellent agreement with

Ref. 26, and our calculated magnetic moment for ferromagnetic $SrRuO_3$ epitaxially constrained to the LDA equilibrium lattice constant of $SrTiO_3$ (less than 0.2% strain) is 1.03 μ_B per Ru atom, consistent with Refs. 27,28,29.

To investigate the response of the heterostructure to an applied electric field, we apply an external bias of ΔV =27.8 mV across the capacitor plates, and allow the ions to relax to their equilibrium positions. The resulting planar and macroscopically averaged change in magnetization is shown in Figure 1. The overall induced magnetic moment is localized at the interfaces, and amounts to 2.5×10^{-3} μ_B per surface unit cell, corresponding to a surface spin density of 0.27 $\mu C/cm^2$. The accumulation of spin is exactly equal in magnitude and opposite in sign (within the numerical accuracy of our method) at the left and right electrode so that the overall induced magnetic moment of the heterostructure is zero, consistent with the symmetry of the system. In the same Figure 1 we show the planar average of the induced spin density without macroscopic averaging. It is clear that the dominant contribution to the induced magnetization is accumulation of spin on the interfacial RuO_2 layer; interestingly, this effect is partially compensated by a smaller *opposite* induced spin density in the adjacent RuO_2 layer, somewhat reminiscent of Kondo behavior[30]. Conversely, the induced spin on the $SrTiO_3$ side of the interface, which is provided by the exponentially vanishing tails of the metal-induced gap states, is small.

Since the magnetoelectric tensor, α, is an intrinsic bulk quantity which relates bulk induced magnetization to applied electric field, it is not the appropriate parameter for describing the interfacial effects observed here. Instead, to characterize the magnetoelectric performance of the device, we start by introducing the notion of *spin-capacitance density* per unit area, $\mathcal{C}_s$ which we define as

$$\mathcal{C}_s = \frac{\sigma_s}{V}, \tag{3}$$

where σ_s is the amount of spin polarization per unit area induced by the voltage V. This definition parallels that of the charge capacitance density per unit area, $\mathcal{C} = \frac{\sigma}{V}$, where σ is the surface density of free charge stored at the electrode. Capacitance densities, however, depend both on the material properties and on the capacitor geometry, in particular, on the thickness of the dielectric film. Therefore, in order to obtain a parameter that characterizes the fundamental properties of the interface response, we further define the

dimensionless parameter η, which is the ratio of spin capacitance to charge capacticance, i.e. $\eta = \mathcal{C}_s/\mathcal{C}$. By definition, η is also equal to the ratio of the induced spin with respect to the free charge accumulated at the capacitor plates, and is clearly zero for non-magnetic electrodes; this interpretation provides a very intuitive picture of the interface response to a field. The spin capacitance of our structure is $\mathcal{C}_s$=96.0 fF/μm^2, to be compared with a charge capacitance of $\mathcal{C}^0$=258 fF/μm^2, yielding a value of η^0=0.37.

In order to investigate the origin of our calculated linear magnetoelectric effect, we first compare this value of $\mathcal{C}^0$ (calculated here by using spin-polarized SRO electrodes) with the value obtained in Ref. 15 for the same system calculated within the non-spin-polarized local density approximation. Strikingly, the two capacitance values are identical within numerical accuracy, indicating that the presence (or absence) of magnetic ordering in the electrode does not influence the dielectric response of the capacitor. The static dielectric response of an insulator can be decomposed into an electronic and an ionic contribution, where the latter is related to the frequency ω_i and the dipolar activity of the zone-center phonons:

$$\epsilon_0 = \epsilon_\infty + \frac{4\pi}{\Omega} \sum_i \frac{Z_i^2}{\omega_i^2} \quad . \tag{4}$$

Here ϵ_∞ is the average frozen-ion permittivity of the supercell, Ω is the volume and Z_i are the "mode effective charges" obtained by summing the ionic Born effective charges weighted by their relative contributions to the normal mode eigenstates. We found no appreciable differences in either ϵ_∞ or the Born effective charges between the non-magnetic and the spin-polarized calculations; the fact that the final value of $\mathcal{C}^0$ is also unaffected strongly suggests that the *frequencies* of the dipolar-active modes are themselves insensitive to magnetism. Therefore, coupling between magnetism and phonons, which has been recognized as a viable route for magnetoelectric switching in perovskite materials[31], is not the driving force for the magnetoelectric response observed here, and a different effect must be responsible.

To elucidate this behavior, we repeat our electric field calculations with the ions frozen in their initial centrosymmetric positions (Figure 2); this isolates the electronic response of the system and corresponds experimentally to the high-frequency limit. Since by keeping the ions fixed we completely remove any structural effect on magnetism, any induced magnetization must be of intrinsic electronic origin, and can only be ascribed to the ca-

pacitive accumulation of spin-polarized carriers at the interface. In this case we obtain an induced magnetic moment at each interface of 1.80×10^{-4} μ_B per unit cell, corresponding to a spin-polarized charge density of 0.019 μC/cm^2, and a high frequency spin capacitance of $\mathcal{C}_s^{\infty}$= 6.99 fF/μm^2. All of these values are an order of magnitude lower than the corresponding quantities in the static case. Indeed the substantially lower induced magnetization and spin capacitance parallel an order of magnitude reduction in the charge capacitance, $\mathcal{C}^{\infty}$=20.3 fF/μm^2, which in turn derives from the suppressed dielectric response of the system when the ions are not allowed to relax. As a consequence, the corresponding value of η^{∞}=0.34 is very close to that obtained in the static case. The similarity in the values of η calculated in the static and high-frequency limits indicates that the mechanisms leading to the screening of polar phonons in the static regime are the same as those screening electronic bound charges in the high-frequency regime, where changes in chemical bonding and/or structure are not possible. Therefore we conclude that our system provides the first example of a *carrier-mediated magnetoelectric effect*, which results entirely from the capacitive accumulation of spin-polarized carriers at the interfaces.

The origin of the carrier-mediated magnetoelectric effect is shown schematically in Figure 3. On application of an external field, free carriers accumulate at the capacitor plates, which are partially screened by the dielectric polarization of the STO film. In the half-metallic limit all displaced electrons are spin-polarized in the same direction (up in the figure); in the present case there is a partial cancellation between spin-up and spin-down carriers that reflects the incomplete spin polarization at the Fermi level of the interfacial SRO layer. This process accumulates up-spin magnetization adjacent to the positively charged electrode, leaving behind an absence of up-spin magnetization (or equivalently down-spin polarized holes) at the negative plate.

One possible mechanism for detecting the induced magnetization is the magneto-optical Kerr effect. Indeed, we note that the recent report of enhanced Kerr response in a 2 nm thick FePt film when an electric field is applied across an electrochemical cell with FePt electrodes[13] is also likely a manifestation of the carrier-mediated magnetoelectric effect that we describe here. In Ref. 13 a Kerr rotation of $\sim 1^{\circ}$ was obtained for an applied potential of 600 mV, which generated 0.015 electrons per unit cell; in our case an equivalent potential would induce a spin polarization of 0.05 spin-polarized electrons per unit cell, which should therefore be readily detectable.

Substitution of our field-polarized dielectric by a ferroelectric with a spontaneous electrical polarization would yield a correspondingly larger spin density and interfacial magnetoelectric effect as well as an added degree of freedom from the switchable polarization. The parameter η has a particularly transparent meaning in this case, relating the accumulated spin at the interface to the bulk polarization of the ferroelectric, P: Neglecting the effect of depolarizing fields (which is a good approximation in the limit of a sufficiently thick ferroelectric film), the free charge accumulated at the electrode exactly compensates the surface polarization charge induced by the spontaneous electric displacement. Therefore, $\eta = \sigma_s/P$, and the induced spin at the interface can be readily predicted by the knowledge of η and P, under the assumption that the behavior of the free carriers is linear in P. For example, from the numbers calculated here we predict σ_s=12 μC/cm^2 for a $SrRuO_3/BaTiO_3$ interface (P_{BTO}=32 μC/cm^2); this corresponds to a fully switchable magnetic moment of 0.11 μ_B. To substantiate these arguments we repeated the calculation by replacing STO with BTO[46]. We restricted our analysis to the high-frequency case to avoid complications related to the proper treatment of BTO lattice instabilities; by analogy with the SRO/STO case, it is unlikely that the fully relaxed static behavior will significantly differ. The resulting $\eta_\infty^{BTO} = 0.37$ is indeed very close to the SRO/STO value, confirming the validity of our arguments. In addition, such ferroelectric/ferromagnetic metal heterostructures would exhibit a new type of *interfacial multiferroism*, resulting from the simultaneous small magnetization of the ferroelectric by the magnetic metal reported in this work, and the polarization of the metallic magnet by the depolarizing field of the ferroelectric described previously in Ref. 15. We note that the interfacial multiferroism results from the attempt by the metallic electrode to screen the capacitive charge at the interface, and is mediated by the capacitive accumlation of spin-polarized carriers at the interfacial layers. The behavior is therefore distinct from that in composite multiferroics, which combine ferro- or ferri-magnetic *insulators* with ferroelectrics (see for example Refs. 9,10,11).

This class of heterostructures was recently investigated by Duan *et al.*[32], who calculated changes in magnetism induced by ferroelectric displacements at the interface between ferroelectric $BaTiO_3$ and ferromagnetic Fe. According to Ref. 32, the positively and negatively polarized faces of the $BaTiO_3$ film have magnetic moments at the interface with the Fe electrodes which differ by almost 0.3 μ_B per surface unit cell; the differences

are ascribed to changes in interfacial chemical bonding and hybridization. While the magnitude of this value is consistent with our estimates, surprisingly most of the change in moment in Ref. 32 resulted from changes in spin polarization of the Ti *d* states, which we find to be minimally affected by the electric field. We note, however, that such changes in hybridization are strongly dependent on the position of Ti *d* states with respect to the Fermi level and can be affected by the well-known underestimation of the fundamental insulating gap that plagues most commonly used DFT functionals. Conversely, the carrier-mediated accumulation of spin-polarized carriers investigated here is a general characteristic of all ferromagnetic electrodes in contact with insulators, regardless of the details of the bonding; since its magnitude is similar to hybridization effects, it should not be neglected.

Finally, we mention some possible related applications that could exploit the predicted carrier-mediated magnetoelectric behavior. With the ability to capacitively store spin-polarized charge, we see that this heterostructure provides the spintronic analogue of a thin film charge capacitor, and could therefore find application in spin-polarized extensions to regular capacitor applications, such as a filter of spin-polarized direct current, or in spin logic circuits. In addition, since the spin capacitance mechanism only allows current to flow when the leads are magnetized in the same direction, the capacitor could be used as a sensitive magnetoresistive detector with the desirable feature that the electrons never cross interfaces and so are less susceptible to scattering of their spin orientation. Since the change in *total* magnetization is small this material combination is not immediately transferable to electric field tunable inductors. The magnitude of the effect would be enhanced, however, by the use of materials with higher spin polarization at the Fermi surface, and lower overall magnetization; in particular half-metallic antiferromagnetic electrodes[33] with zero net magnetization would give an infinite relative change in net magnetization with electric field. We note also that the calculated LSDA dielectric constant of $SrTiO_3$ is 490, whereas experimental values can be tens of thousands, and the induced magnetization will scale accordingly.

To summarize, we have used first-principles density functional calculations combined with finite electric field methods to demonstrate a linear magnetoelectric response in a complex oxide heterostructure. This new carrier-mediated mechanism adds an additional degree of freedom in the design and functionalization of magnetoelectric multi-

ferroic materials, and may guide the way forward in designing electric-field switchable magnetic devices. With growing interest in superlattice multiferroic composites, the phenomenon we describe may elucidate experimentally observed effects that to date are attributed to unknown interfacial responses to applied electric (and magnetic) fields[34]. Our results also expand the growing body of literature demonstrating the novel functionality that can be achieved at oxide interfaces[12,35,36,37,38,39,40,41] and suggest an additional route to novel oxide-based interfacial devices[42].

This work was supported by the DOE SciDac program on Quantum Simulations of Materials and Nanostructures, grant number DE-FC02-06ER25794 (M.S.), and by the NSF NIRT program, grant number 0609377 (J.M.R). N.S. thanks the Miller Institute at UC Berkeley for their support through a Miller Research Professorship.

---

* Address correspondence to: nicola@mrl.ucsb.edu; *Competing Interests.* The authors declare that they have no competing financial interests.

1 O'Dell, T. *The Electrodynamics of Magneto-Electric Media* (North-Holland, Amsterdam, 1970).

2 Fiebig, M. Revival of the magnetoelectric effect. *J. Phys. D: Appl. Phys.* **38**, R1–R30 (2005).

3 Dzyaloshinskii, I. On the magneto-electric effect in antiferromagnets. *Soviet Phys. J. Expt. Theor. Phys.* **10**, 628629 (1960).

4 Astrov, D. The magnetoelectric effect in antiferromagnetics. *Soviet Phys. J. Expt. Theor. Phys.* **11**, 708709 (1960).

5 Binek, C. & Doudin, B. Magnetoelectronics with magnetoelectrics. *J. Phys.: Condens. Matter* **17**, L39–L44 (2005).

6 Borisov, P., Hochstrat, A., Chen, X., Kleemann, W. & Binek, C. Magnetoelectric switching of exchange bias. *Phys. Rev. Lett.* **94**, 117203 (2005).

7 Wang, J. *et al.* Epitaxial $BiFeO_3$ multiferroic thin film heterostructures. *Science* **299**, 1719 (2003).

8 Kimura, T. *et al.* Magnetic control of ferroelectric polarization. *Nature* **426**, 55–58 (2003).

9 Srinivasan, G. *et al.* Magnetoelectric bilayer and multilayer structures of magnetostrictive and piezoelectric oxides. *Phys. Rev. B* **64**, 214408 (2001).

10 Zheng, H. *et al.* Multiferroic $BaTiO_3$-$CoFe_2O_4$ nanostructures. *Science* **303**, 661–663 (2004).

11 Dong, S., Cheng, J., Li, J. F. & D.Viehland. Enhanced magnetoelectric effects in laminate com-

posites of terfenol-D/Pb(Zr,Ti)O_3 under resonant drive. *Appl. Phys. Lett.* **83**, 4812–4814 (2003).

[12] Yamada, H. *et al.* Engineered interface of magnetic oxides. *Science* **305**, 646–648 (2004).

[13] Weisheit, M. *et al.* Electric field-induced modification of magnetism in thin-film ferromagnets. *Science* **315**, 349–351 (2007).

[14] Stengel, M. & Spaldin, N. A. Ab-initio theory of metal-insulator interfaces in a finite electric field. *Phys. Rev. B* **75**, 205121 (2007).

[15] Stengel, M. & Spaldin, N. A. Origin of the dielectric dead layer in nanoscale capacitors. *Nature* **443**, 679–682 (2006).

[16] Velev, J. P. *et al.* Negative spin polarization and large tunneling magnetoresistance in epitaxial Co—$SrTiO_3$—Co magnetic tunnel junctions. *Phys. Rev. Lett.* **95**, 216601 (2005).

[17] Marrec, F. L. *et al.* Magnetic behavior of epitaxial $SrRuO_3$ thin films under pressure up to 23 GPa. *Appl. Phys. Lett.* **80**, 2338–2340 (2002).

[18] Ahn, C. H. *et al.* Ferroelectric field effect in ultrathin $SrRuO_3$ films. *Appl. Phys. Lett.* **70**, 206–208 (1997).

[19] Takahashi, K. S. *et al.* Local switching of two-dimensional superconductivity using the ferroelectric field effect. *Nature* **441**, 195–198 (2006).

[20] Gallagher, W. J. & Parkin, S. S. P. Development of the magnetic tunnel junction MRAM at IBM: from first junctions to a 16-Mb MRAM demonstrator chip. *IBM J. Res. Dev.* **50**, 5–23 (2006).

[21] Blöchl, P. E. Projector augmented-wave method. *Phys. Rev. B* **50**, 17953–17979 (1994).

[22] Monkhorst, H. J. & Pack, J. D. Special points for brillouin-zone integrations. *Phys. Rev. B* **13**, 5188–5192 (1976).

[23] Car, R. & Parrinello, M. Unified approach for molecular dynamics and density-functional theory. *Phys. Rev. Lett.* **55**, 2471–2474 (1985).

[24] VandeVondele, J. & A. De Vita. First-principles molecular dynamics of metallic systems. *Phys. Rev. B* **60**, 13241 (1999).

[25] Stengel, M. & De Vita, A. First-principles molecular dynamics of metals: A Lagrangian formulation. *Phys. Rev. B* **62**, 15283–15286 (2000).

[26] Antons, A., Neaton, J. B., Rabe, K. M. & Vanderbilt, D. Tunability of the dielectric response of epitaxially strained $SrTiO_3$ from first principles. *Phys. Rev. B* **71**, 024102 (2005).

[27] Allen, P. B. *et al.* Transport properties, thermodynamic properties, and electronic structure of $SrRuO_3$. *Phys. Rev. B* **53**, 4393–4398 (1996).

[28] Singh, D. J. Electronic and magnetic properties of the 4d itinerant ferromagnet $SrRuO_3$. vol. 79, 4818–4820 (AIP, 1996).

[29] Mazin, I. I. & Singh, D. J. Electronic structure and magnetism in Ru-based perovskites. *Phys. Rev. B* **56**, 2556–2571 (1997).

[30] Kondo, J. Anomalous hall effect and magnetoresistance of ferromagnetic metals. *Prog. Theor. Phys.* **27**, 772 (1962).

[31] Fennie, C. J. & Rabe, K. M. Magnetic and electric phase control in epitaxial $EuTiO_3$ from first principles. *Phys. Rev. Lett.* **97**, 267602 (2006).

[32] Duan, C.-G., Jaswal, S. S. & Tsymbal, E. Y. Predicted magnetoelectric effect in $Fe/BaTiO_3$ multilayers: Ferroelectric control of magnetism. *Phys. Rev. Lett.* **97**, 077204 (2006).

[33] Pickett, W. E. Spin-density-functional-based search for half-metallic antiferromagnets. *Phys. Rev. B* **57**, 10613–9 (1998).

[34] Chaudhuri, A. R., Ranjith, R., Krupanidhi, S. B., Mangalam, R. V. K. & Sundaresan, A. Interface dominated biferroic $La_{0.6}Sr_{0.4}MnO_3/0.7Pb(Mg_{\frac{1}{3}}Nb_{\frac{2}{3}})O_3$–$0.3PbTiO_3$ epitaxial superlattices. *Appl. Phys. Lett.* **90**, 122902 (2007).

[35] Ohtomo, A., Muller, D. A., Grazul, J. L. & Hwang, H. Y. Artificial charge-modulation in atomic-scale perovskite titanate superlattices. *Nature* **419**, 378–380 (2002).

[36] Ohtomo, A. & Hwang, H. Y. A high-mobility electron gas at the $LaAlO_3/SrTiO_3$ heterointerface. *Nature* **427**, 423–426 (2004).

[37] Thiel, S., Hammerl, G., Schmehl, A., Schneider, C. W. & Mannhart, J. Tunable quasi-two-dimensional electron gases in oxide heterostructures. *Science* **313**, 1942–1945 (2006).

[38] Hwang, H. Y. Tuning interface states. *Science* **313**, 1895–1896 (2006).

[39] Huijben, M. *et al.* Electronically coupled complementary interfaces between perovskite band insulators. *Nature Materials* **5**, 556–560 (2006).

[40] De Teresa, J. M. *et al.* Role of metal-oxide interface in determining the spin polarization of magnetic tunnel junctions. *Science* **286**, 507–509 (1999).

[41] Lottermoser, T. *et al.* Magnetic phase control by an electric field. *Nature* **430**, 541–544 (2004).

[42] Kroemer, H. Nobel lecture: Quasielectric fields and band offsets: teaching electrons new tricks. *Rev. Mod. Phys.* **73**, 783–793 (2001).

[43] Zhao, T. *et al.* Electrically controllable antiferromagnets: Nanoscale observation of coupling between antiferromagnetism and ferroelectricity in multiferroic $BiFeO_3$. *Nature Mater.* **5**, 823 –

829 (2006).

[44] Although not strictly a linear magnetoelectric effect, a related behavior in single-phase multiferroics, in which electric field re-orientation of ferroelectric polarization reorients the magnetic easy axis or plane through the elastic coupling[43] and vice versa[8], has recently received considerable attention.

[45] The PAW pseudopotentials were generated in the $4s^2 4p^6 5s^2$ configuration for Sr, $3s^2 3p^6 4s^2 3d^2$ for Ti, $2s^2 2p^4$ for O and $4s^2 4p^6 4d^7 5s^1$ for Ru.

[46] Six Sr atoms within the insulating layer were replaced with Ba, which corresponds to assuming a TiO_2 (SrO) termination of the BTO (SRO) lattice. The in-plane lattice parameter was kept fixed to the calculated bulk STO value, while both out-of-plane lattice parameter and atomic positions were fully relaxed while imposing mirror symmetry with respect to a plane parallel to the interface.

Figures

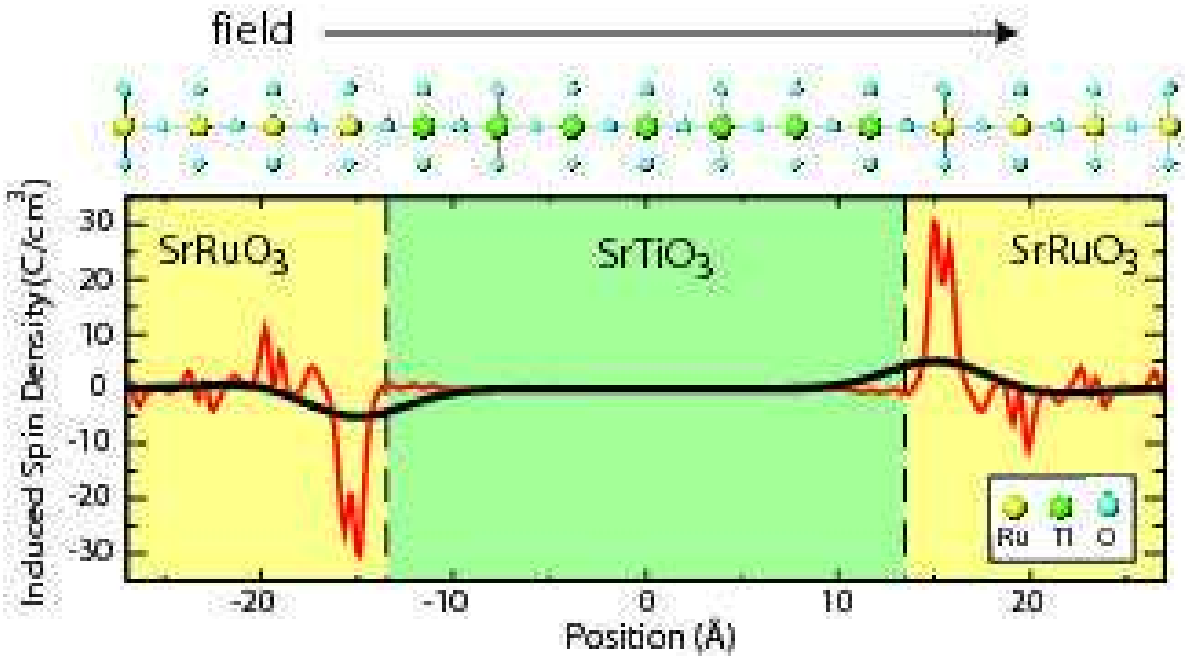

FIG. 1: (color online) Calculated magnetization induced by an external voltage of 27.8 mV in a nanocapacitor consisting of 7 layers of $SrTiO_3$ alternating with 7 layers of ferromagnetic, metallic $SrRuO_3$. The light (red) and bold (black) lines show respectively the planar averaged, and macroscopically and planar averaged induced magnetization profiles.

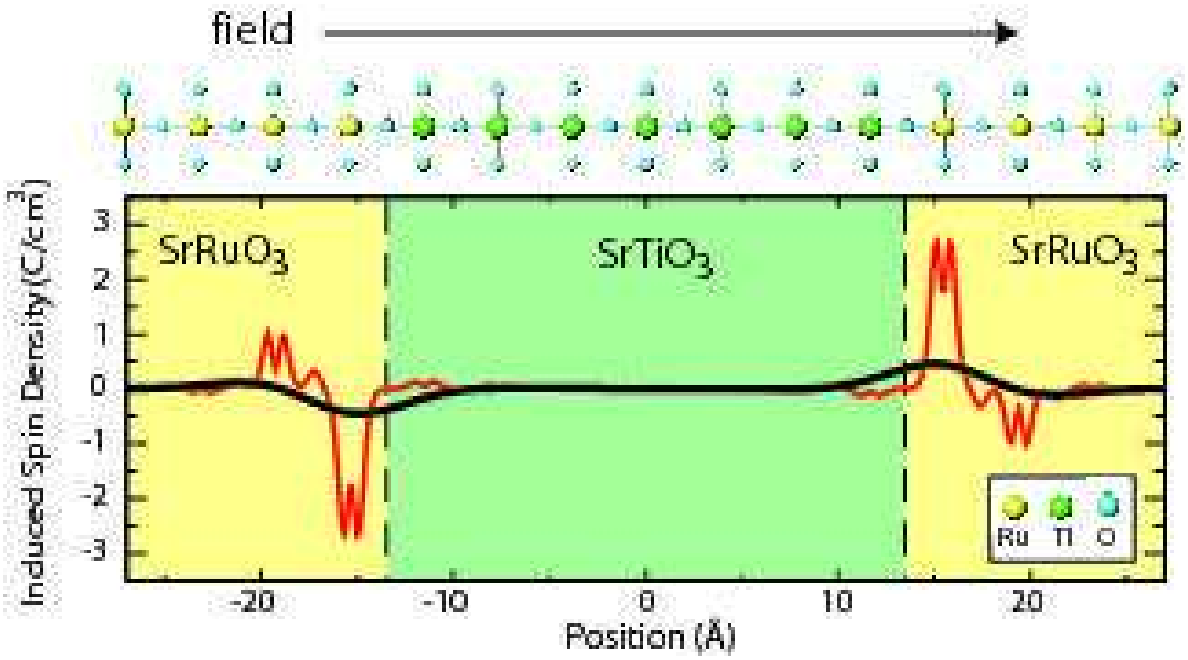

FIG. 2: (color online) Calculated high-frequency planar averaged magnetization induced by an external voltage of 27.8 mV. The light (red) and bold (black) lines show respectively the planar averaged, and macroscopically and planar averaged profiles. Note that the y-axis scale is exactly one order of magnitude smaller than in the static case (Fig. 1). The strong change in local spin density on the interfacial Ru atoms is evident, along with a small local magnetic moment on the interfacial Ti atoms.

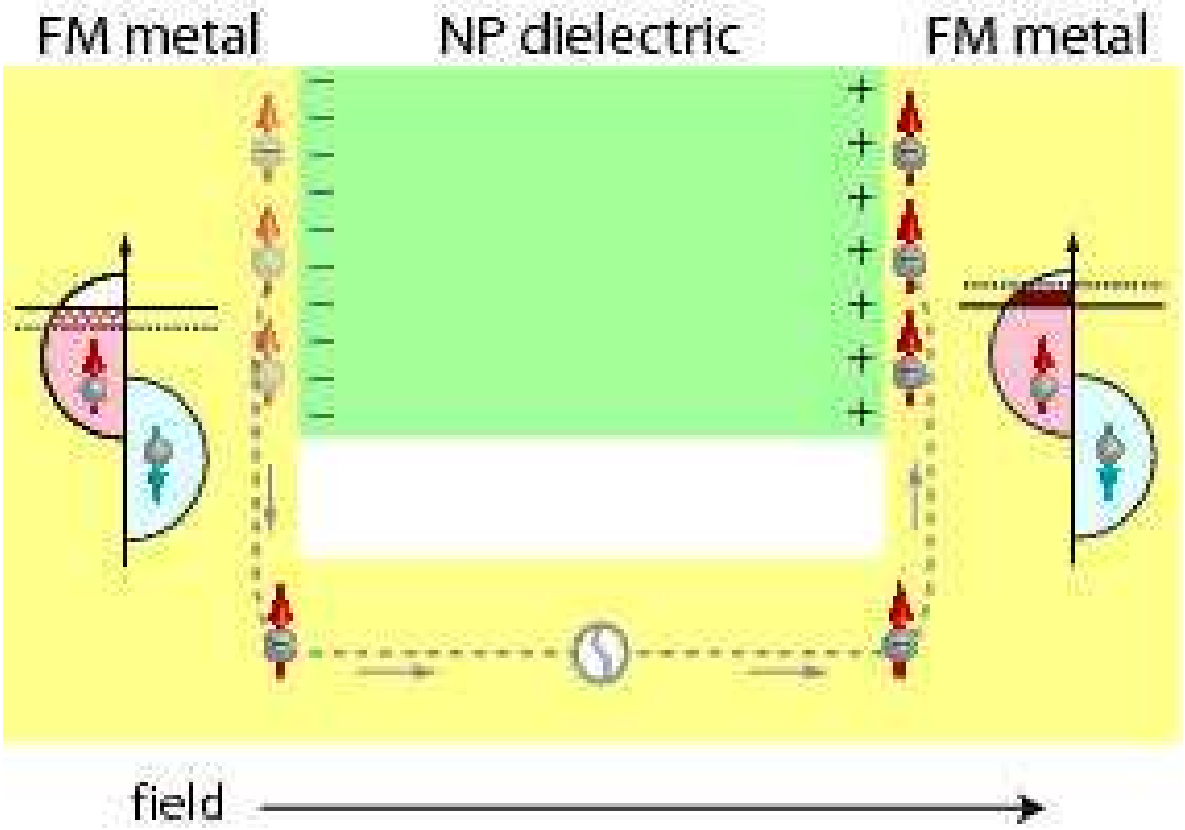

FIG. 3: (color online) Schematic of the mechanism causing the induced magnetization at a ferromagnetic (FM) metal – non-polar (NP) dielectric interface. The inset density of states cartoons show the changes to the occupation of half-metallic densities of states in the electrodes when the current flows in response to the applied electric field. The accumulation of up-spin electrons adjacent to the positive face of the dielectric, and their depletion from the negative face, leads to the net magnetization shown in Figs. 1 and 2.

Tables

	magnetic non-polar	non-magnetic polar	magnetic polar	magnetic interface
time-reversal symmetric?	no	yes	no	no
space-inversion symmetric?	yes	no	no	no
linear ME effect allowed?	no	no	yes	yes

TABLE I: The linear magneto-electric (ME) effect is only allowed in the absence of both time-reversal and space-inversion symmetries. For a single phase material the co-existence of electrical polarization and magnetic ordering are required for linear magneto-electricity to occur; in the presence of an interface which breaks space-inversion symmetry the existence of magnetic ordering is sufficient.